

## Supplementary Information

### Cucurbit[7]uril-based carbon dots for recognizing histamine

Jian-Hang Hu, Cheng-Hui Wang, Qing-Hong Bai, Li-Xia Chen, An-Ting Zhao, Shang-

Wei Yuan, Qing Chen, Pei-Hua Ma, Zhu Tao and Xin Xiao\*

*National Key Laboratory of Green Pesticide, State Key Laboratory of Green Pesticide and Agricultural Bioengineering, Ministry of Education, Key Laboratory of Macrocyclic and Supramolecular Chemistry of Guizhou Province, Guizhou University, Guiyang 550025, China.*

E-mail: gyhxxiaoxin@163.com or xxiao@gzu.edu.cn (Xin Xiao).

## Contents

<b>1. Materials and instruments</b> .....	4
1.1 Materials .....	4
1.2 Instruments .....	4
<b>2. Experimental method</b> .....	4
2.1 <sup>1</sup> H NMR spectroscopy .....	5
2.2 Isothermal titration calorimetry (ITC) experiment .....	5
2.3 Fourier transform infrared spectroscopy (FTIR) experiment .....	5
2.4 Single crystal X-ray crystallography .....	6
2.5 Preparation of complex 1 .....	6
2.6 Preparation of fluorescence spectrum (FL) solution .....	7
2.7 Synthesis and purification of Q[7]-CDs .....	7
2.8 Detection of Biogenic amine by Q[7]-CDs .....	7
2.9 Preparation of real samples.....	8
Figure S1. Structures of Q[7] and DMPA. ....	8
Figure S2. <sup>1</sup> H NMR spectra (400 MHz, D <sub>2</sub> O) of DMPA and the presence of Q[7].....	9
Figure S3. ITC profile of host Q[7] with guest DMPA at 298.15K. ....	9
Figure S4. Identifiable thermal ellipsoid plots for all non-hydrogen atoms.....	10
Figure S5. Q[7]-DMPA thermogravimetric analysis plot. ....	10
Figure S7. fluorescence responses of the Q[7]-CQDs in different pH solutions.....	11
Figure S8. FT-IR spectra of the Q[7], Q[7]-DMPA and DMPA.....	12
Figure S9. particle size distributions of the Q[7]-CQDs. ....	12
Figure S10. Scanning electron microscopy analysis of the Q[7]-CQDs. ....	13
Figure S11. High resolution spectra of N1s; (d) high resolution spectra of O1s.....	14
Figure S12. High resolution spectra of O1s; .....	14
Figure S13. Emission spectra of each biogenic amine, amine substances and possible interference. ....	15
Figure S14. the Detection Limit (DL) of the Q[7]-CQDs for histamine. ....	15
Figure S15. Fluorescence spectra of Q[7]-CQDs-His and Q[7]-CQDs-His with other 23 substances ((1-25 are Q[7]-CQDs, Histamine, Tyramine, Amylaceum, Putrescine, S <sup>2-</sup> , SO <sub>3</sub> <sup>2-</sup> , N-propyl, Cadaverine, L-cysteine, Phenylethylamine, NO <sup>2</sup> , Glutathione, SO <sub>4</sub> <sup>2-</sup> , Cl <sup>-</sup> , NO <sup>3-</sup> , Hydrazine hydrate, Pyridine, Aqueous ammonia, N,N-Dimethylethy-lenediamine,	

Trimethylamine, Ethylamine, Dimethylamine, Triethyl-amine and Hydroxylamine hydrochloride, respectively). .....	16
Figure S16. (a) <sup>1</sup> H NMR spectrum of DMPA; (b) <sup>1</sup> H NMR spectrum of Q[7]-CQDs; (c) <sup>1</sup> H NMR spectrum of Q[7]-CQDs with Histamine; (d) <sup>1</sup> H NMR spectrum of Histamine. ....	17
Figure S17. UV-vis absorption spectra of Q[7]-CQDs and fluorescence emission spectra of the histamine. ....	17
Table S1. ITC measurements of the thermodynamics of Q[7]-DMPA interaction at 298.15 K .....	17
Table S2. Assignments of the Bands of the Infrared Absorption Spectra for Q[7]-CDS.....	18
Table S3. Crystal data and structure refinement for Q[7]-DMPA.....	18
Table S4. The determination of His spiked in real samples. ....	20
<b>References</b> .....	21

## **1. Materials and instruments**

### **1.1 Materials**

We purchased 2,2-Bis(hydroxymethyl)propionic acid from Aladdin in Shanghai, China. Following the recommended approach in the literature, Q[7] was created and purified. [1] Basiji shrimp, black carp and pork purchased from MeiTuan Online Fresh Supermarkets (China), red wine purchased from China Agri-Foods Group (COFCO) Great Wall Wine (China). The use of the other reagents required no additional purification because they were of analytical reagent grade. All trials utilized deionized water.

### **1.2 Instruments**

A JEOL JNM-ECZ400S nuclear magnetic resonance spectrometer (Japan Electronics Corporation, 400MHz) was used to record  $^1\text{H}$  NMR. Isothermal titration calorimetry (ITC) experiments were carried out with a Nano ITC instrument (TA, USA) apparatus at 25°C. Fluorescence emission spectra were recorded on a VARIAN Cary Eclipse spectrofluorometer (Varian, Inc., Palo Alto, CA, USA) and VARIOSKAN LUX (Thermo Fisher Scientific, USA). The High Resolution TEM (HRTEM) image were recorded on a FEI Tecnai G2 F20 High Resolution Transmission Electron Microscope. scanning electron microscope (SEM) were recorded on a ZEISS GeminiSEM 300 (German). Single-crystal data for compound **1** were collected on the Bruker D8 VENTURE diffractometer with graphite monochromatic Mo-K $\alpha$  radiation ( $\lambda = 0.71073$  Å). Dynamic light scattering (DLS) was performed on a Malvern Nano ZS90 (England). Thermogravimetric analysis by means of the Netzsch Simultaneous Thermal Analyzer STA 449 F5 (Germany).

## **2. Experimental method**

## 2.1 <sup>1</sup>H NMR spectroscopy

All the <sup>1</sup>H NMR spectra, including those for the titration experiments, were recorded at 298.15 K on a JEOL JNM-ECZ400S 400 MHz NMR spectrometer (JEOL) in D<sub>2</sub>O. D<sub>2</sub>O was used as a field-frequency lock and the observed chemical shifts are reported in parts per million (ppm) relative to that for the internal standard (TMS at 0.0 ppm). To investigate the complexation of Q[7] with 2,2-Bis(hydroxymethyl)-propionic acid in solution, <sup>1</sup>H NMR spectroscopic titration experiments were performed by adding increasing amounts of Q[7] to the solution of DMPA in D<sub>2</sub>O.

## 2.2 Isothermal titration calorimetry (ITC) experiment

To further understand the nature of host-object complexation of Q[7] with 2,2-bis(hydroxymethyl)propionic acid, isothermal titration calorimetry (ITC) experiments were performed. The obtained thermodynamic parameters reveal that the host-guest complexation is enthalpically favourable. In addition to the ion-dipole interaction between the positively charged nitrogens on the 2,2-Bis(hydroxymethyl)propionic acid guest and the oxygen atoms on the portals of the Q[7] host, van der Waals interaction between the surfaces of the 2,2-Bis(hydroxymethyl)propionic acid guest and the inner wall of the Q[7] host contribute favourable enthalpy for the host-guest complexation. This favorable entropic gain is probably the result of the removal of the water molecules from the 2,2-Bis(hydroxymethyl)propionic's solvated shell, Q[7] cavity, and Q[7] portals.

## 2.3 Fourier transform infrared spectroscopy (FTIR) experiment

The above Q[7]-CDs and spectrally pure potassium bromide were dried in a vacuum drying oven and mixed at a ratio of about 1 : 200. The mixture was thoroughly ground and mixed in an agate mortar, and then the tablets were pressed on a pressure machine for sample preparation using the matching mold of an infrared spectrometer.

The absorption/transmission spectrum was recorded by an infrared spectrometer with a scanning range of 400-4000  $\text{cm}^{-1}$

## 2.4 Single crystal X-ray crystallography

The temperature was 298.15K. Empirical absorption corrections were applied by using the multi-scan program SADABS-2016/2 (Bruker,2016/2). R(int) was 0.2324 before and 0.095 after correction. The Ratio of minimum to maximum transmission is 0.6973. The  $\lambda/2$  correction factor is Not present. Structural solution and full-matrix least-squares refinement based on  $F^2$  were performed within the program Olex2. [2] Anisotropic thermal parameters were applied to all the non-hydrogen atoms. All hydrogen atoms were treated as riding atoms with an isotropic displacement parameter equal to 1.2 times that of the parent atom. The disordered solvent was modelled using a solvent mask within Olex2. For some other crystal-related data, please refer to the supporting information in Table S1.

CCDC: 2224143 contains the supplementary crystallographic data for this paper. These data can be obtained free of charge via [www.ccdc.cam.ac.uk/data\\_request/cif](http://www.ccdc.cam.ac.uk/data_request/cif), by emailing [data\\_request@ccdc.cam.ac.uk](mailto:data_request@ccdc.cam.ac.uk), or by contacting The Cambridge Crystallographic Data Centre, 12, Union Road, Cambridge CB21EZ, UK (fax: +44 1223-336033).

## 2.5 Preparation of complex 1

Q[7] (6.71 mg, 0.005 mmol) was added to a solution of 2,2-Bis(hydroxymethyl)-propionic acid (6.7 mg, 0.05 mmol),  $\text{CdCl}_2$  (9.2 mg, 0.05 mmol) and  $\text{CaCl}_2$ (5.5mg, 0.05mmol) in HCl solution (5 mL, 3  $\text{mol}\cdot\text{L}^{-1}$ ). The mixture was heated until complete dissolution. Following slow evaporation of the volatiles from the solution over a period of about three days, block colourless crystals of complex 1 were obtained.

## 2.6 Preparation of fluorescence spectrum (FL) solution

3 mL of 200 mg/mL solution was transferred into a fluorescence colorimetric dish, and the fluorescence emission spectrum of the Q[7]-CDs was measured by fluorescence spectrophotometer. The fluorescence emission spectra of the carbon quantum dot solution in each centrifuge tube excited at 340 nm were measured.

## 2.7 Synthesis and purification of Q[7]-CDs

DMPA (6.7 mg, 0.05 mM) and Q[7] (67.1 mg, 0.05 mM) were dissolved in deionized water (50 mL). The solution was stirred for 60 min and the solution was transferred into a Teflon autoclave. After being heated at 180 °C for 12 h, the autoclave was cooled to room temperature. The reaction solution was centrifuged at 4000 rpm for 45 min, and the supernatant was collected. The resulting supernatant is further filtered through an organic membrane with a cut-off flow rate of 1000 KDa and a flattened width of 22 mm to remove large or agglomerated particles. After removing the solvents and freeze-drying, a brown powder was obtained (40 mg, yield 48%).

## 2.8 Detection of Biogenic amine by Q[7]-CDs

Different biogenic amine, amine substances and possible interference (Amylaceum, Tyramine, Histamine, Putrescine, *N*-propyl, Cadaverine, *L*-cysteine, Phenylethylamine, Glutathione, Hydrazine hydrate, Pyridine, Aqueous ammonia, *N,N*-Dimethylethylenediamine, Trimethylamine, Ethylamine, Dimethylamine, Triethylamine, Hydroxylamine hydrochloride,  $S^{2-}$ ,  $SO_3^{2-}$ ,  $NO_2^-$ ,  $SO_4^{2-}$ ,  $Cl^-$ ,  $NO_3^-$ ) were added into the prepared fluorescent probe standard solution (3 mL of 200 mg/mL) for detection (the added amino acid concentration is 0.02 mol/L, and the volume is 50  $\mu$ L). The fluorescence emission spectra of the carbon quantum dot solution in each centrifuge tube excited at 340 nm were measured, and the change of fluorescence intensity was compared with that of blank solution without the biogenic amine.

## 2.9 Preparation of real samples

The basiji shrimp, black carp, pork samples with a blender, respectively, weighing mixed samples 10.0 g in a stoppered conical flask, add 100 mL of water, cover the stopper, ultrasonic shaking at room temperature for 30 min, filtration. The above filtrate was centrifuged (3000 r) in an EP tube for 10 min and the supernatant was taken and set aside. 3 mL of the extract was taken and different concentrations of histamine standard samples were added to it.

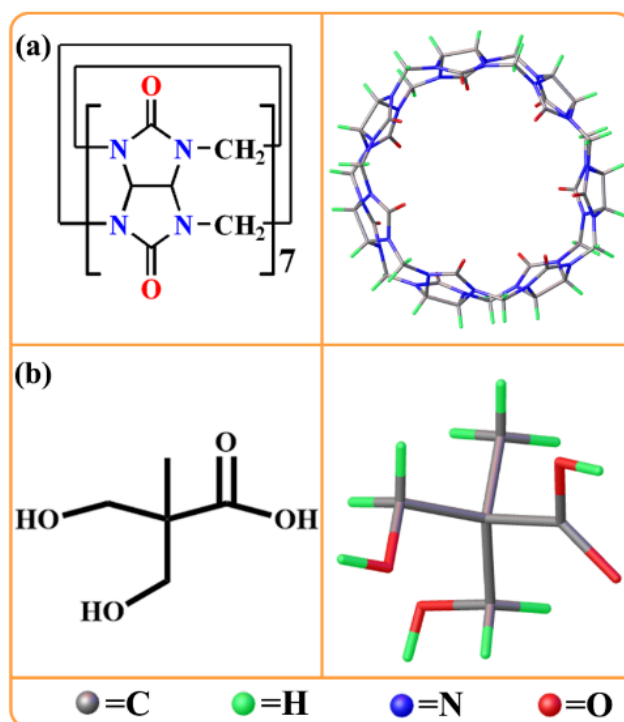


Figure S1. Structures of Q[7] and DMPA.



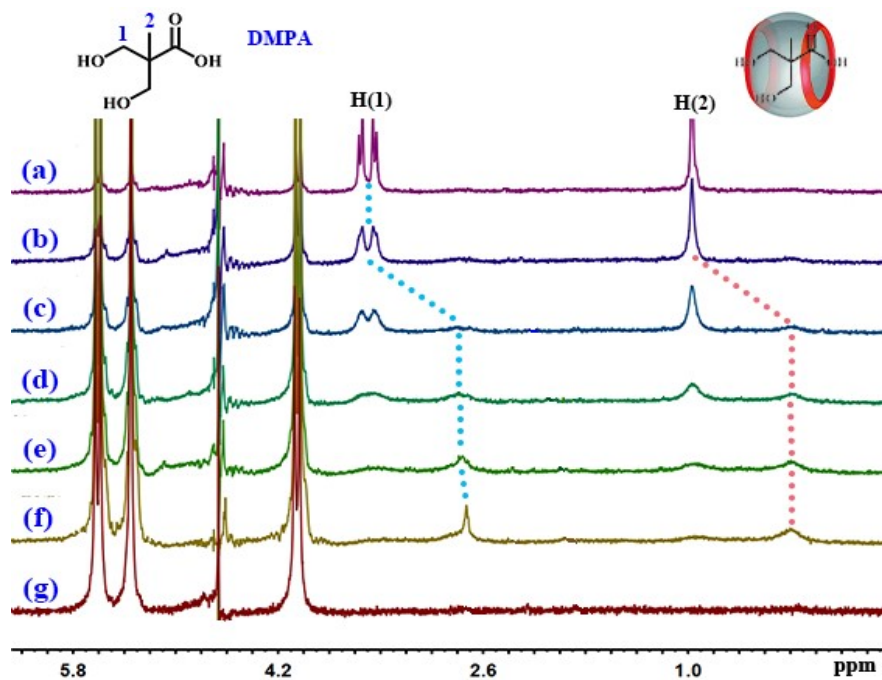


Figure S2.  $^1\text{H}$  NMR spectra (400 MHz,  $\text{D}_2\text{O}$ ) of DMPA and the presence of Q[7].

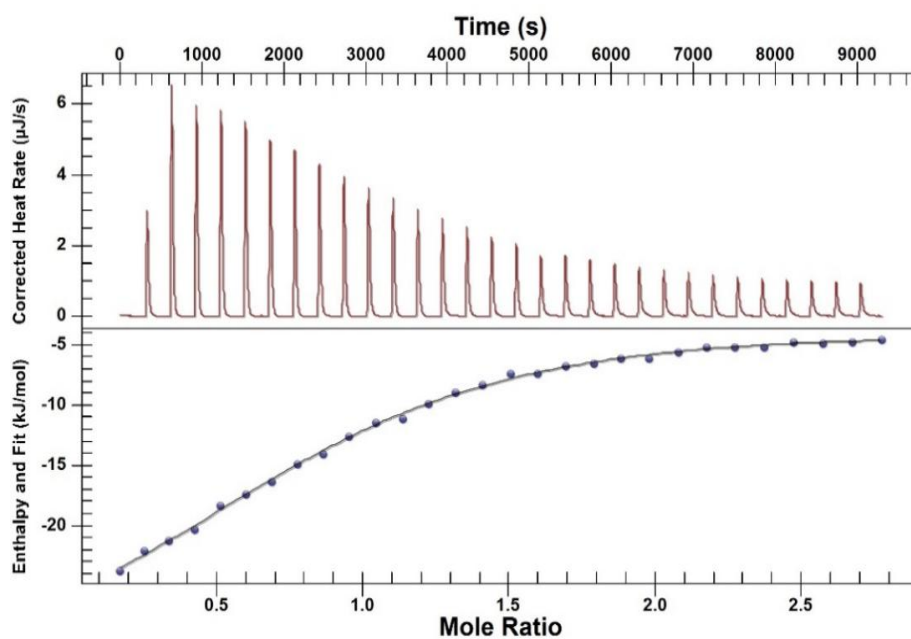


Figure S3. ITC profile of host Q[7] with guest DMPA at 298.15K.

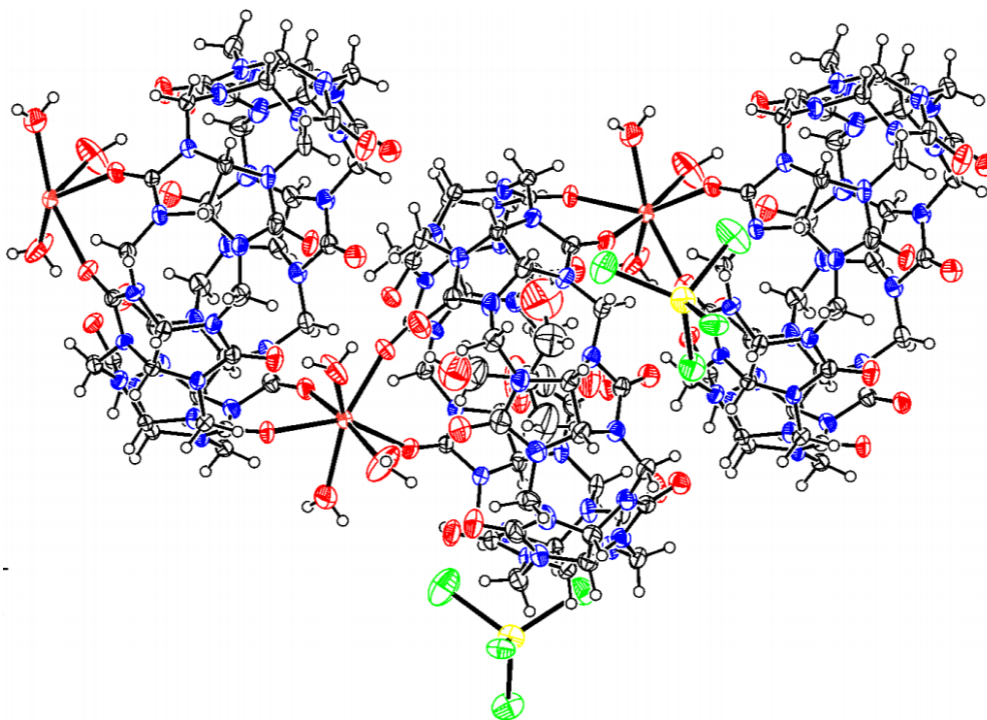


Figure S4. Identifiable thermal ellipsoid plots for all non-hydrogen atoms.

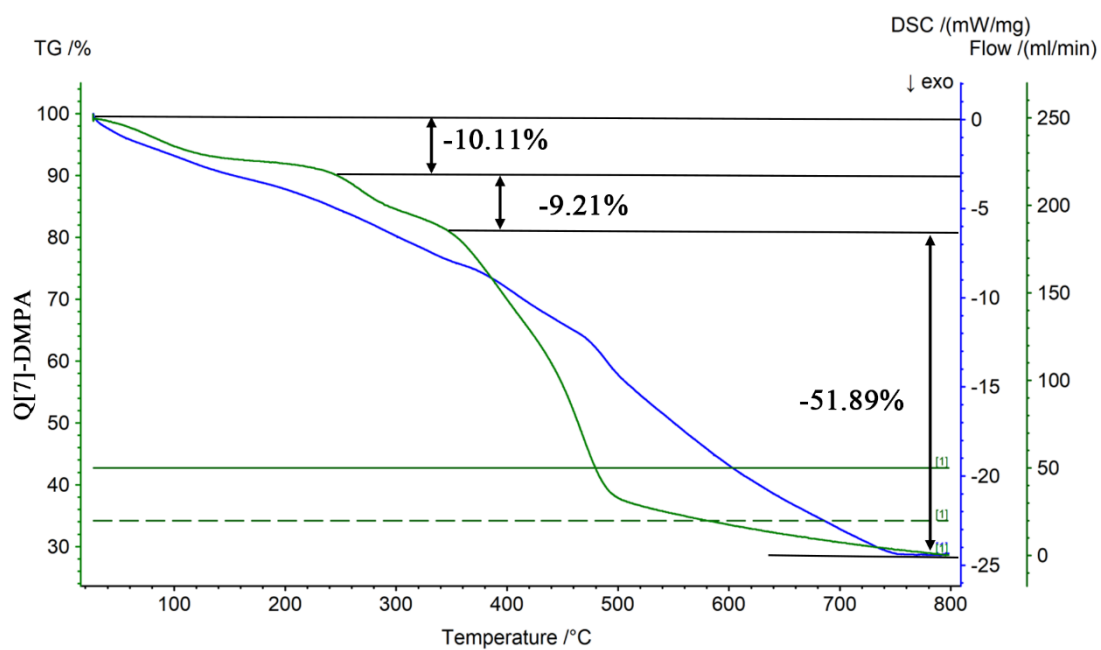


Figure S5. Q[7]-DMPA thermogravimetric analysis plot.

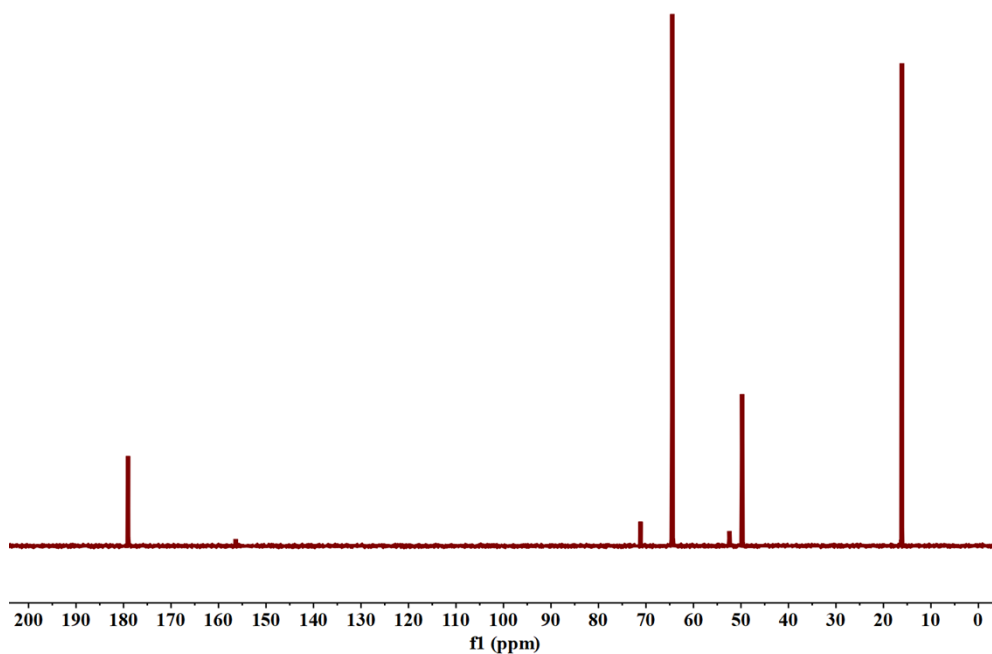


Figure S6.  $^{13}\text{C}$  NMR spectrum of Q[7]-CQDs

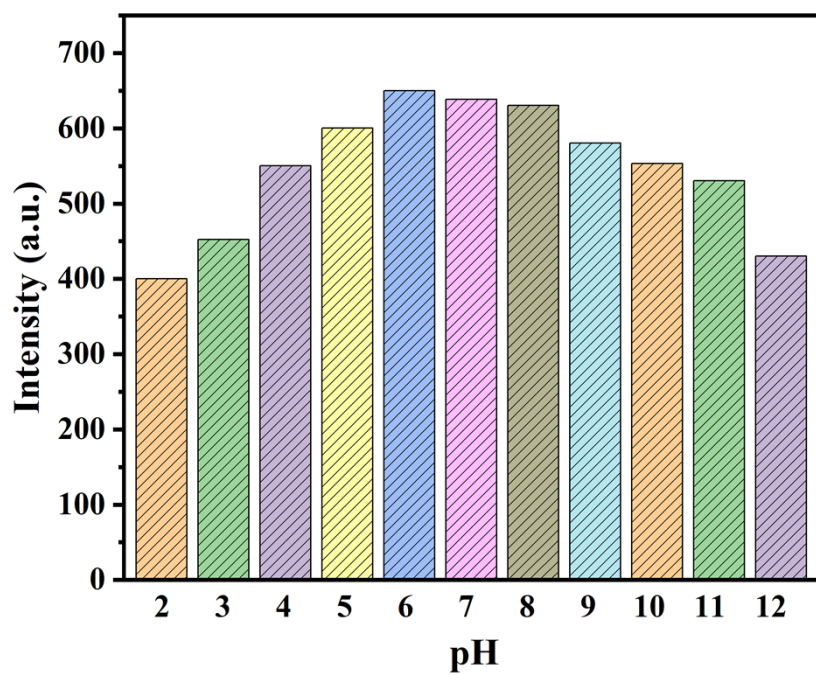


Figure S7. fluorescence responses of the Q[7]-CQDs in different pH solutions.

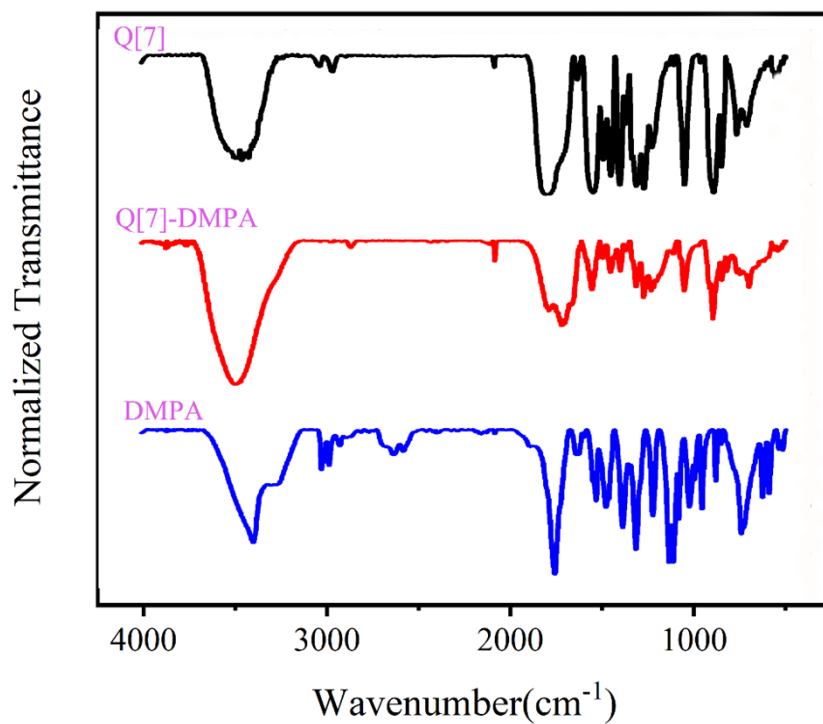


Figure S8. FT-IR spectra of the Q[7], Q[7]-DMPA and DMPA.

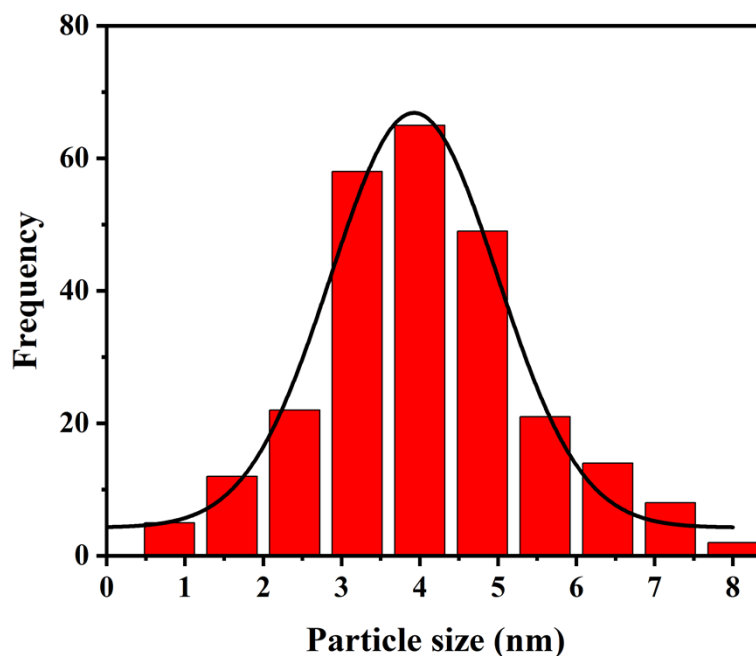
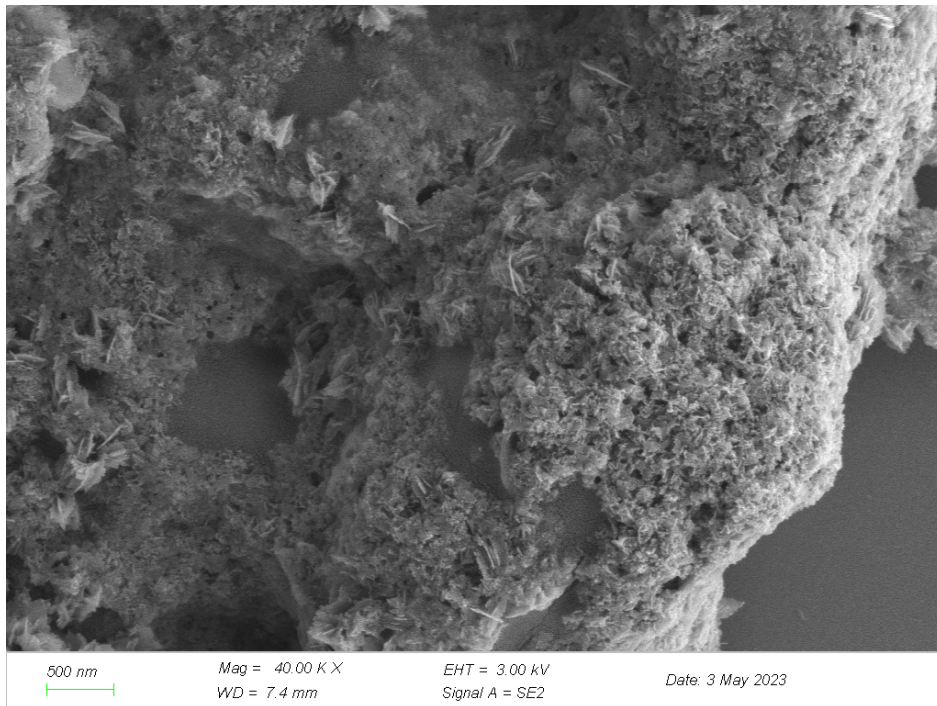


Figure S9. particle size distributions of the Q[7]-CQDs.



**Figure S10. Scanning electron microscopy analysis of the Q[7]-CQDs.**

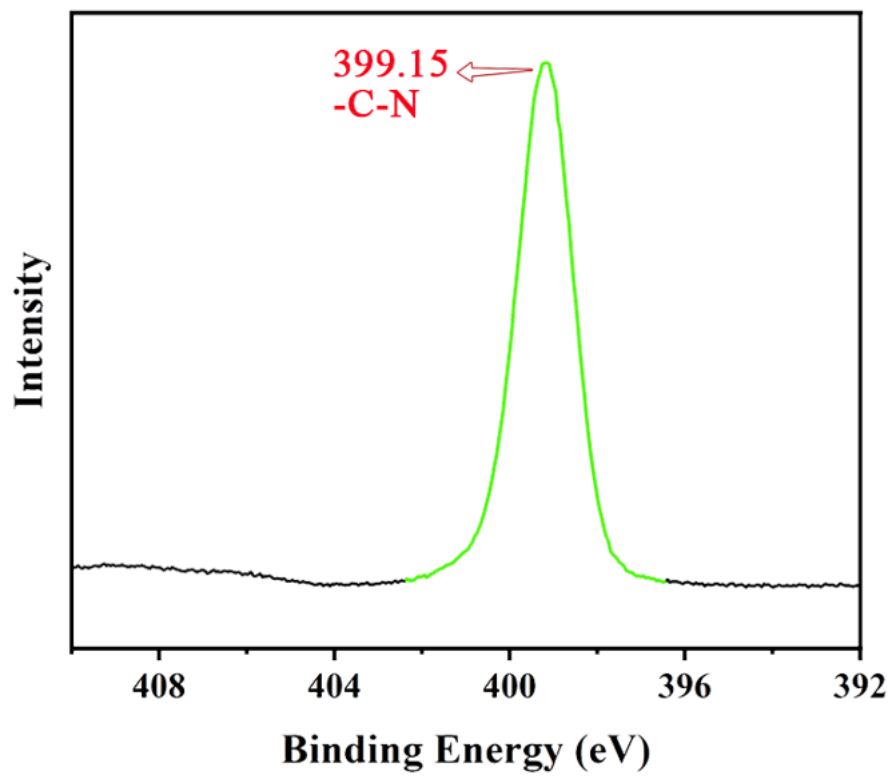


Figure S11. High resolution spectra of N1s; (d) high resolution spectra of O1s.

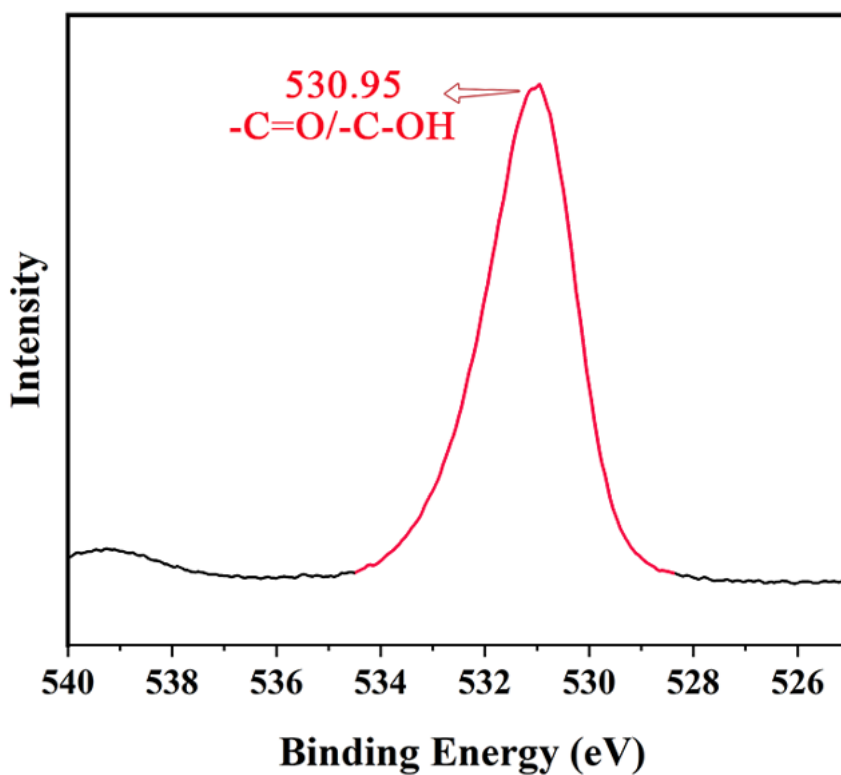


Figure S12. High resolution spectra of O1s;

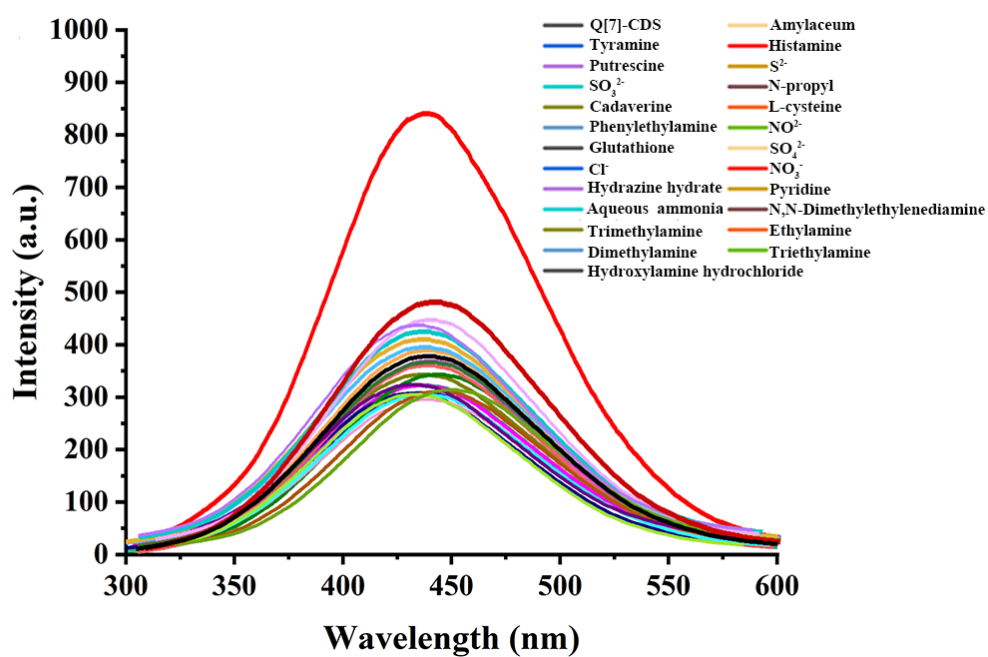


Figure S13. Emission spectra of each biogenic amine, amine substances and possible interference.

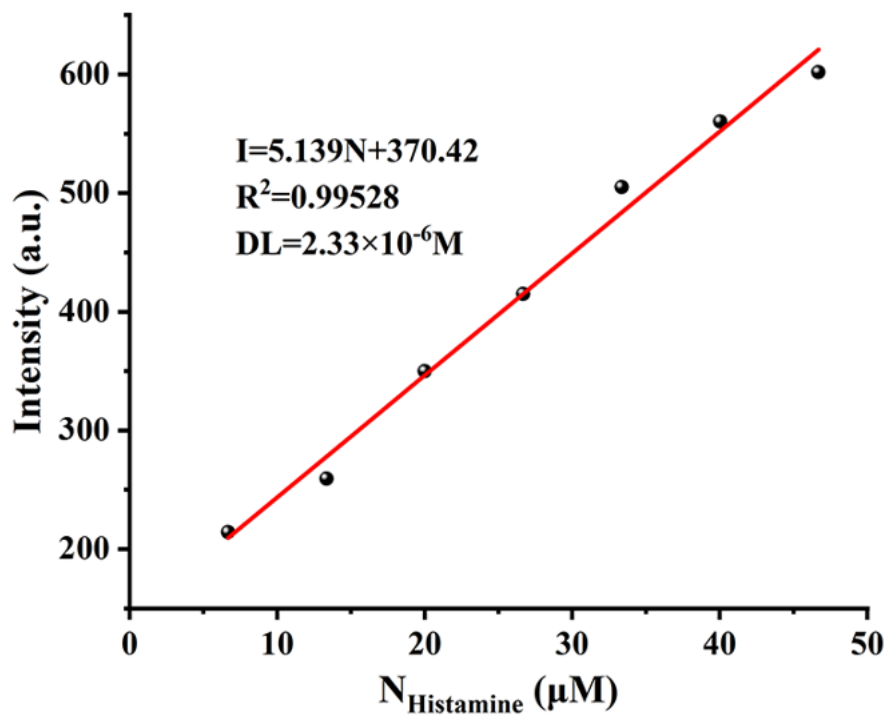


Figure S14. the Detection Limit (DL) of the Q[7]-CQDs for histamine.

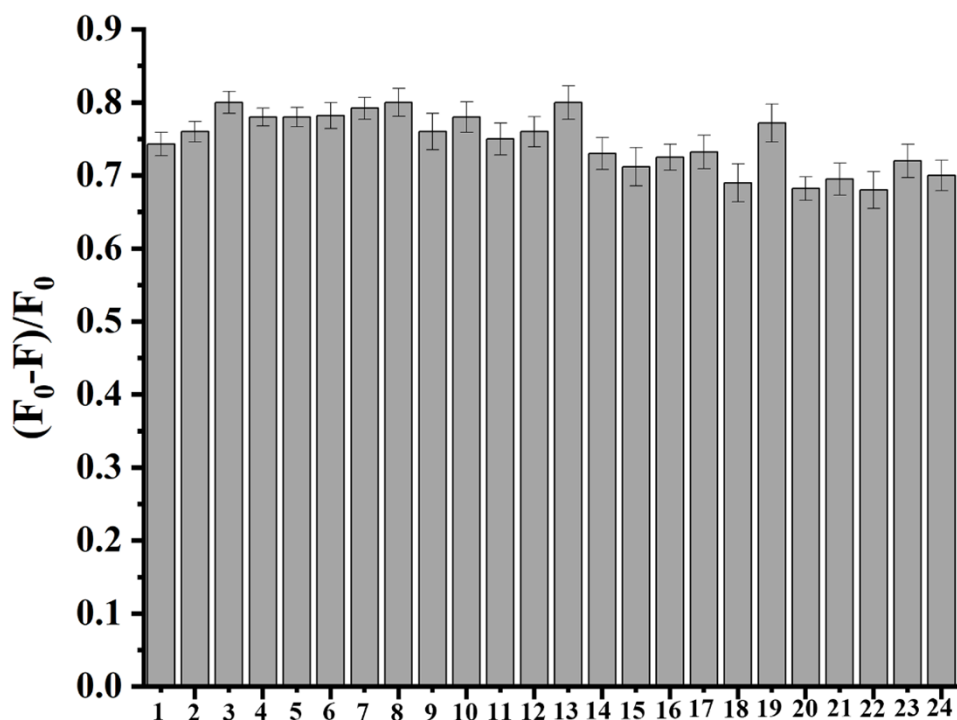


Figure S15. Fluorescence spectra of Q[7]-CQDs-His and Q[7]-CQDs-His with other 23 substances ((1-25 are Q[7]-CQDs, Histamine, Tyramine, Amylaceum, Putrescine,  $S^{2-}$ ,  $SO_3^{2-}$ , N-propyl, Cadaverine, L-cysteine, Phenylethylamine,  $NO^2$ , Glutathione,  $SO_4^{2-}$ ,  $Cl^-$ ,  $NO^3^-$ , Hydrazine hydrate, Pyridine, Aqueous ammonia, N,N-Dimethylethy-lenediamine, Trimethylamine, Ethylamine, Dimethylamine, Triethyl-amine and Hydroxylamine hydrochloride, respectively).

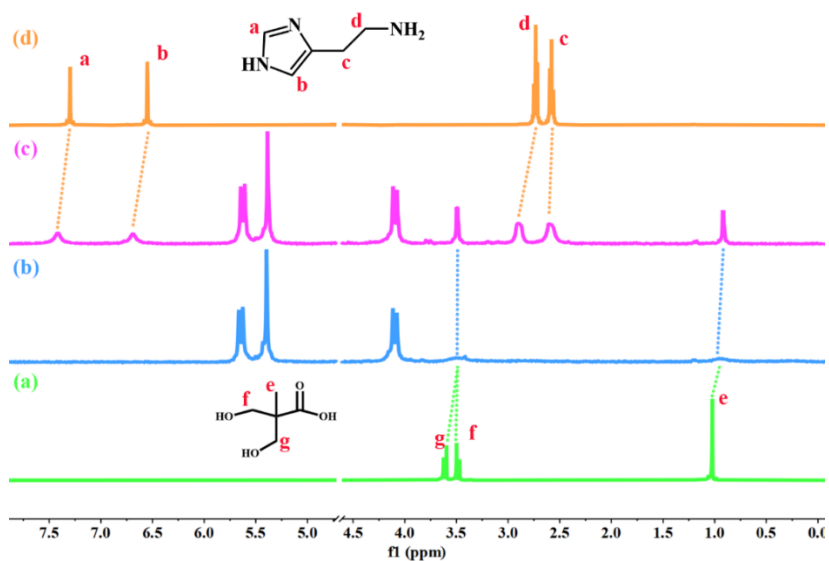




Figure S16. (a)  $^1\text{H}$  NMR spectrum of DMPA; (b)  $^1\text{H}$  NMR spectrum of Q[7]-CQDs; (c)  $^1\text{H}$  NMR spectrum of Q[7]-CQDs with Histamine; (d)  $^1\text{H}$  NMR spectrum of Histamine.

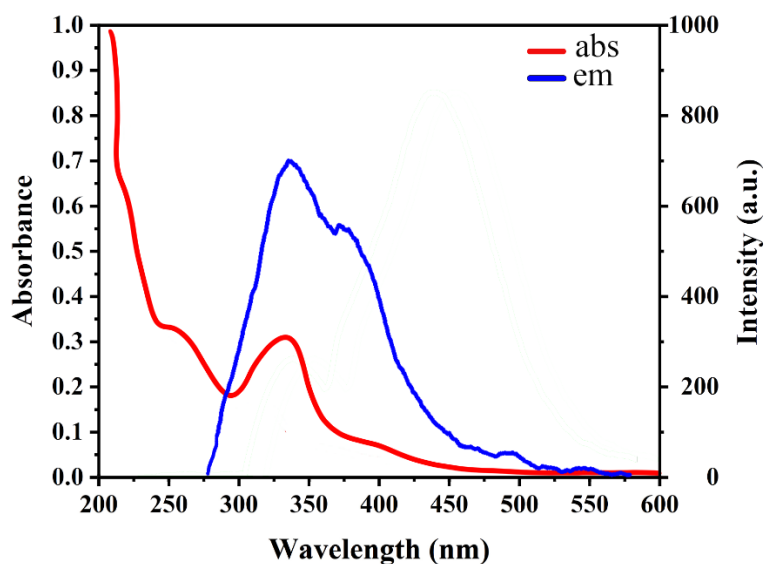


Figure S17. UV-vis absorption spectra of Q[7]-CQDs and fluorescence emission spectra of the histamine.

Table S1. ITC measurements of the thermodynamics of Q[7]-DMPA interaction at 298.15 K

Experiment	Q[7]@ DMPA
$K_a$ ( $\text{M}^{-1}$ )	$3.38 \times 10^4$
$\Delta H$ ( $\text{kJ} \cdot \text{mol}^{-1}$ )	-35.32
$T\Delta S$ ( $\text{kJ} \cdot \text{mol}^{-1}$ )	-9.896
$\Delta G$ ( $\text{kJ} \cdot \text{mol}^{-1}$ )	-25.42
$\Delta S$ ( $\text{kJ} \cdot \text{mol}^{-1}$ )	-33.76

n	0.911
---	-------

**Table S2. Assignments of the Bands of the Infrared Absorption Spectra for Q[7]-CDS.**

Observed IR (cm <sup>-1</sup> )	Attributions
3468	$\nu(\text{O-H})$
2826	$\nu(\text{C-H})$
1721	$\nu(\text{C=O})$
1645	$\nu_s(\text{C=O})$
1483	$\delta_s(\text{C-H})$
1419	$\nu(\text{CH}_2), \nu(\text{CH}_3)$
1378	$\delta_s(\text{CH}_3)$
1323	$\beta(\text{CH}_2) + \omega(\text{CH}_2)$
1234	$\nu_s(\text{C-N})$
1192	$\nu(\text{C-H}), \nu(\text{all nucleus})$
1146	$\nu(\text{C-C})$
968	$\beta(\text{C-H})$
806	$\gamma(\text{C-C-H})$
756	$\nu(\text{CH}_2), \nu(\text{C-H}), \nu(\text{C-N})$
607	$\beta(\text{O-H})$

**Table S3. Crystal data and structure refinement for Q[7]-DMPA.**

Empirical formula	$\text{C}_{47}\text{H}_{57}\text{CaCd}_2\text{Cl}_8\text{N}_{28}\text{O}_{21}$
Formula weight	1898.68

Temperature/K	273.15
Crystal system	monoclinic
Space group	P2 <sub>1</sub> /n
a/Å	16.852(3)
b/Å	17.108(3)
c/Å	29.168(6)
$\alpha$ /°	90
$\beta$ /°	94.92(3)
$\gamma$ /°	90
Volume/Å <sup>3</sup>	8378(3)
Z	4
$\rho_{\text{calc}}$ /cm <sup>3</sup>	1.505
$\mu$ /mm <sup>-1</sup>	0.901
F(000)	3820.0
Crystal size/mm <sup>3</sup>	0.22 × 0.15 × 0.12
Radiation	MoK $\alpha$ ( $\lambda$ = 0.71073)
2 $\Theta$ range for data collection/°	4.536 to 60.774
Index ranges	-23 ≤ h ≤ 18, -23 ≤ k ≤ 24, -41 ≤ l ≤ 41
Reflections collected	254259
Independent reflections	25102 [ $R_{\text{int}}$ = 0.0809, $R_{\text{sigma}}$ = 0.0450]
Data/restraints/parameters	25102/9/972
Goodness-of-fit on F <sup>2</sup>	1.018
Final R indexes [ $I \geq 2\sigma(I)$ ]	$R_1$ = 0.0950, $wR_2$ = 0.2502
Final R indexes [all data]	$R_1$ = 0.1112, $wR_2$ = 0.2604

**Table S4. The determination of His spiked in real samples.**

Sample	Spiked ( $\mu\text{M}$ )	Fluorescent sensing system		
		Found	Recovery (n=5, %)	RSD (n=5, %)
basiji shrimp	20	18.64 $\pm$ 0.58	93.2 $\pm$ 2.9	2.23
	40	39.56 $\pm$ 0.83	98.9 $\pm$ 2.1	1.52
	60	60.73 $\pm$ 0.33	101.2 $\pm$ 0.5	1.93
black carp	20	21.65 $\pm$ 1.23	108.2 $\pm$ 6.15	3.21
	40	40.13 $\pm$ 1.12	100.3 $\pm$ 2.8	2.95
	60	61.06 $\pm$ 1.54	101.7 $\pm$ 2.5	2.89
pork	20	19.36 $\pm$ 1.01	96.8 $\pm$ 5.1	1.55
	40	38.96 $\pm$ 1.52	97.4 $\pm$ 3.8	0.96
	60	59.87 $\pm$ 1.35	99.7 $\pm$ 2.3	1.38
Red wine	20	18.96 $\pm$ 1.55	94.8 $\pm$ 7.75	1.52
	40	38.38 $\pm$ 2.03	95.95 $\pm$ 5.10	1.36
	60	57.96 $\pm$ 2.13	96.6 $\pm$ 3.55	1.25

## References

- [1] H.-Y. Wang, Y. Zhou, J.-H. Lu, Q.-Y. Liu, G.-Y. Chen, Z. Tao, Xin Xiao, Supramolecular Drug Inclusion Complex of Capecitabine with Cucurbit[7]uril and Inverted Cucurbit[7]uril, *Arabian Journal of Chemistry* 13(1) (2020) 2271-2275.
- [2] O. V. Dolomanov, L. J. Bourhis, R. J. Gildea, J. A. K. Howard, H. Puschmann, OLEX2: a complete structure solution, refinement and analysis program, *Journal of Applied Crystallography* 42(2) (2009) 339-341.